Published in final edited form as:
Cell Host Microbe. 2013 March 13; 13(3): 314–323. doi:10.1016/j.chom.2013.02.008.

Defining Influenza A Virus Hemagglutinin Antigenic Drift by Sequential Monoclonal Antibody Selection

Suman R. Das[1,2,3], **Scott E. Hensley**[1,5], **William L. Ince**[1], **Christopher B. Brooke**[1], **Anju Subba**[2], **Mark G. Delboy**[2], **Gustav Russ**[4], **James S. Gibbs**[1], **Jack R. Bennink**[1], and **Jonathan W. Yewdell**[1,*]

[1]Laboratory of Viral Diseases, NIAID, Bethesda, MD 20892, USA

[2]Infectious Diseases Group, J. Craig Venter Institute, Rockville, MD 20850, USA

[3]Emory Vaccine Center, Emory University, Atlanta, GA 30322, USA

[4]Institute of Virology, Slovak Academy of Sciences, 84505 Bratislava, Slovak Republic

SUMMARY

Human influenza A virus (IAV) vaccination is limited by “antigenic drift,” rapid antibody-driven escape reflecting amino acid substitutions in the globular domain of hemagglutinin (HA), the viral attachment protein. To better understand drift, we used anti-hemagglutinin monoclonal Abs (mAbs) to sequentially select IAV escape mutants. Twelve selection steps, each resulting in a single amino acid substitution in the hemagglutinin globular domain, were required to eliminate antigenicity defined by monoclonal or polyclonal Abs. Sequential mutants grow robustly, showing the structural plasticity of HA, although several hemagglutinin substitutions required an epistatic substitution in the neuraminidase glycoprotein to maximize growth. Selecting escape mutants from parental versus sequential variants with the same mAb revealed distinct escape repertoires, attributed to contextual changes in antigenicity and the mutation landscape. Since each hemagglutinin mutation potentially sculpts future mutation space, drift can follow many stochastic paths, undermining its unpredictability and underscoring the need for drift-insensitive vaccines.

INTRODUCTION

Influenza A virus (IAV) is a major public health concern, on a yearly basis costing the USA alone upwards of $50 billion while killing tens of thousands (Molinari et al., 2007). Although current vaccines lessen the burden of influenza, they are far less effective than vaccines for other similar viral pathogens. This is due to the ability of IAV to modulate its antigenicity on a yearly basis. This process, termed antigenic drift, reflects the accumulation

*Correspondence: jyewdell@niaid.nih.gov.
[5]Present address: The Wistar Institute, Philadelphia, PA 19130, USA

ACCESSION NUMBERS

The GenBank accession numbers for the WT and mutant influenza A virus (A/PR/8/1934 H1N1) genome sequences (full length and partial) reported in this paper are CY084006, CY084007, CY084008, CY084009, CY0840010, CY084011, CY084012, CY084013, CY038895, CY038896, CY038897, CY038898, CY038899, CY038900, CY038901, CY038902, CY038903, CY038904, CY038905, CY038906, CY038907, CY038908, CY038909, CY038910, CY105896, CY105897, CY105898, CY105899, CY105900, CY105901, CY105902, CY105903, CY105904, CY105905, CY105906, CY105907, CY105908, CY105909, CY105910, CY105911, CY105912, CY105913, CY105914, CY105915, CY105916 CY105917, CY105918, CY105919, CY105920, CY105921, CY105922, CY105923, CY105924, CY105925, CY105926, CY105927, CY105928, CY105929, CY105930, CY105931, CY105932, CY105933, CY105934, CY105935, CY105936, CY105937, CY105938, CY105939, CY105940, CY105941, and CY105942.

SUPPLEMENTAL INFORMATION

Supplemental Information includes one figure and three tables and can be found with this article at http://dx.doi.org/10.1016/j.chom.2013.02.008.

of amino acid substitutions in the globular domain of HA (Webster et al., 1975), the principal target of Abs that neutralize IAV infectivity.

HA initiates the infectious cycle by binding terminal sialic acid (SA) residues on target cells and mediating the fusion of viral and cellular membranes. Sequencing escape mutants of A/PR/8/34 (H1N1) (PR8) selected by neutralizing monoclonal Abs (mAbs) (Caton et al., 1982; Gerhard et al., 1981) revealed five largely nonoverlapping immunodominant antigenic sites. Sa and Sb (strain specific) are located at the tip of the globular domain, while Ca_1 and Ca_2 and Cb (crossreactive) are located toward the stem of H1 HA. Based largely on the correlation of antigenic sites with the degree of variation observed in drifted field isolates, it is believed that "drift" results strictly from antigenic escape. Recent results, however, suggest that selection for other factors, such as HA receptor specificity and avidity, and epistatic interactions within HA and with neuraminidase (NA) and other IAV gene products can select for changes in the globular region that alter antigenicity (Hensley et al., 2009, 2011; Kryazhimskiy et al., 2011).

Thus, although antigenic drift of IAV has been known for nearly 80 years (Francis et al., 1947), the relative contribution of various selective factors is uncertain. An important but largely ignored question is why IAV rapidly drifts while other RNA viruses (e.g., paramyxoviruses) with equivalent mutation rates and frequency of mAb escape mutants do not (van Wyke Coelingh et al., 1987; Yewdell and Gerhard, 1982). To what extent is drift due to (1) Special features of IAV transmission in human populations or the interaction of IAV with individual hosts? (2) Enhanced ability of HA to accept amino acid substitutions and change antigenicity while maintaining full functionality? (3) The ability of IAV to buffer changes in HA function with epistatic changes in other genes, e.g., NA, a process facilitated by the segmented nature of the IAV genome?

Here, we address the characteristics of IAV that favor antigenic drift by sequentially selecting IAV escape mutants with mAbs until escape from a large panel of neutralizing mAbs is complete.

RESULTS

In Vitro Modeling of Drift by Generating Sequential Variants

The H1 HA has five spatially distinct immunodominant antigenic sites, but single amino acid substitutions at each site only abrogate the binding of a fraction of Abs specific for each site (Caton et al., 1982; Gerhard et al., 1981). How many substitutions are required to completely abrogate antigenicity defined by polyclonal Abs and a large panel of mAbs induced by WT virus?

We addressed this question by sequentially selecting mutants with a panel of mAbs (Table 1). After each selection step, we measured antigenicity using a large panel of mAbs via radioimmunoassay (RIA) and then repeated the process with a mAb that demonstrated little or no alteration in affinity for the sequential variant. Loss of antigenicity was gradual and predictable based on the relationship between the epitopes recognized by the selecting Ab and the queried panel Ab. (Figure 1A). Twelve selection steps were required to reduce binding at least 10-fold to all but 4 of a 182 member mAb panel (Table 1, the remaining mAbs demonstrate weak neutralization/hemagglutination inhibition [HI] activity [Yewdell, 1981]).

The reactivity of mAbs paralleled the reactivity of mouse pAbs in mouse serum following primary or booster immunization as measured by HI (Table 2). Postinfection ferret antisera (from multiple sources), the WHO/CDC standard used for gauging antigenic drift in

epidemic viruses, showed a similar decrease to the sequential (SEQ-) variants (Table 2). Sera from guinea pig, rabbits, and birds (chickens) all showed substantial incremental decreases with the SEQ variants, suggesting similarities in the recognition of the globular domain by Ab responses among vertebrate species (Table 2).

To examine the ability of SEQ-12 to escape immunity in vivo, we vaccinated B6 mice with inactivated PR8 virus, intranasally challenged them 3 weeks later with PR8 and SEQ-12 mixed at approximately a 5:1 ratio, and harvested lungs 2 days later (Table S1). Immunization with inactivated virus resulted in a 10-fold reduction in viral titer ($p = 0.018$, Student's t test). Comparison of SEQ-12 and PR8 variant frequencies in immunized mice clearly demonstrates that SEQ-12 outcompetes PR8 despite starting at a 1:5 ratio ($p < 0.0001$ Fisher's exact test), whereas in naive mice PR8 has a slight growth advantage over SEQ-12 ($p = 0.03$), thus confirming an overall clear growth advantage of SEQ-12 in vaccinated mice.

These findings demonstrate that HA undergoes gradual, step-by-step antigenic drift when confronted with individual mAbs, and that the panel we used is relevant for escape in mice, guinea pigs, rabbits, chickens, and ferrets, and likely humans as well, based on the predictive value of ferret reference sera in gauging significant antigenic drift (Smith et al., 2004).

Sequential Variants Exhibit Epistatic Changes in NA Related to Optimizing Receptor Avidity

Sequencing of the sequential panel revealed that each selection step was accompanied by a single nonsynonymous mutation encoding a residue in the predicted antigenic site for each selecting mAb (Table 1, located on the HA structure in Figure 1B). For most variants, there were no additional changes in either HA or the seven other IAV gene segments. The lack of reversion or addition of epistatic changes in these viruses suggests that viral fitness was not greatly affected by the selection process. Consistent with this finding, the frequency of mAb H36-84 escape mutants in the SEQ-11 and WT stocks were indistinguishable ($10^{-6.2}$), demonstrating that escape was not increasingly constrained by the ability of the HA to accept novel mutations after 11 selection steps. Sequential variants all grew to similarly high titers in eggs (see Figure S1 online).

Three of the SEQ- variants possessed a nonsynonymous mutation in the NA gene, resulting in a G357S substitution (H5N1 numbering-based NA crystal structure 2HTY, G339S; based on PR8 numbering, starting from initiating Met) (Figure 1C). This mutation appeared in SEQ-8 and persisted until reverting in SEQ-11. Although the reversion suggests that the mutation is not a random "hitchhiker" offering no selective advantage, we examined its evolutionary value by comparing the abilities of WT and mutant NA genes to complement WT versus mutant HAs based on virus titer after rescue and growth in MDCK cells (Figure S1). This revealed a clear preference of the SEQ-8 (and possibly SEQ-9 HA, p value = 0.28, also a slightly lower success rate for rescuing virus) for mutant versus WT NA. Conversely, WT HA or SEQ-7 HA did not demonstrate a significant preference for mutant versus WT NA, confirming that the mutant NA is selected to enhance the growth of SEQ variants.

When assessed on a per particle basis (assessed by hemagglutination activity), the G357S substitution reduced NA activity as measured using a simple fluorogenic substrate (Figure 2A). Activity differences occurred independently of glycoprotein organization in virions, since they persisted when virus was disrupted by adding triton X 100. When NA activity was normalized to NA protein amount in virions, no differences were observed between WT and mutant, indicating that the mutation does not reduce NA activity (Figure 2B). Instead, by analyzing virion protein content, we found that the G357S substitution markedly reduces the amount of NA incorporated into virus particles relative to HA (Figure 2C).

The reduction in per particle NA activity in SEQ variants was associated with increased HA receptor avidity, measured by resistance of viral HA activity to removal of terminal sialic residues by bacterial NA (Yewdell et al., 1986). Increased avidity first appeared in SEQ-7 and peaked in SEQ-8, where the NA mutation was first detected (Figure 2D). E156K, appearing in SEQ-7, also increases receptor avidity in a single mAb escape mutant (Hensley et al., 2009), while E119K, the mutation in SEQ-8, is in the same location as E119G, also known to increase receptor avidity as a single substitution (Hensley et al., 2009).

This finding emphasizes the importance of optimal HA avidity for virus growth, and the ability of epistatic changes in NA to compensate for suboptimal HA function, as we recently reported (Das et al., 2011; Hensley et al., 2011). Substitutions in SEQ-9, SEQ-10, and SEQ-11 all diminish HA avidity, reinforcing the surprising conclusion that residues quite distant from the classical receptor-binding site (residue 48, altered in SEQ-11, is located on the opposite face of the HA, more than 50 Å from the receptor-binding site) can influence receptor binding (Hensley et al., 2009). That SEQ-11 was accompanied by a reversion in NA (rather than an epistatic change in another NA residue) strongly suggests that NA has little mutational latitude in compensating for the altered function of the G357S mutation. Notably, position 357 is highly conserved among N1 genes: in 791 isolates from 1,934 to 2,000 curated at the influenza research database (http://www.fludb.org/), there are but 10 isolates with substitutions (G357N or G357D). Based on the crystal structure of a related N1 NA, residue 357 is located on the “underside” of the globular head ~25 Å from the active site (Figure 1C), likely explaining the unchanged enzymatic activity. Rather, our evidence implicates this residue in controlling the efficiency of NA incorporation into virions.

Together, these data show that, as predicted by our previous study (Hensley et al., 2009), the receptor properties of HA are altered by immune escape-driven mutations in the classic antigenic sites, some of which require compensatory NA mutations to restore fitness.

Sequential Variants Demonstrate Novel Amino Acid Substitutions

All of the SEQ- substitutions are located in the sites expected for their respective selecting mAb (Table 1 and Figure 1B). Remarkably, however, when compared to a panel of single selection mutants (Caton et al., 1982; Yewdell et al., 1993), three substitutions represent novel changes at a given position (depicted in blue), while two of the substitutions are present in entirely novel positions (depicted in red).

This suggested that the “escape space” of HA changes as it accumulates amino acid substitutions. To test this hypothesis, we used two mAbs with highly similar epitopes in the Ca site, H17-L2 and H17-L10 (Ca8 and Ca6, respectively, in Gerhard et al., 1981) to compare the PR8 and SEQ-7 repertoires of mutants that escape from neutralization. H17-L10 was used to select the unique mutation in SEQ-9 (Table 1). Both mAbs utilize γ2a heavy chains and κ light chains, and require HA trimerization to create their epitopes (Yewdell et al., 1988), consistent with their epitopes spanning the trimer interface (Figure 3). These two mAbs recognize PR8 and SEQ-7 with similar affinity (Figures 4D and 4E) and exhibit similar neutralization and HI potency (Table S2).

Analysis of large panels of escape mutants revealed the selection of many distinct mutants (Table 3 and Table S3). The large discrepancy in the frequency of individual mutations (ranging from less than 1% to more than 80%) is almost certainly due to differences in viral fitness, as such large differences are inconsistent with relatively minor differences in codon degeneracy of the frequencies of individual base substitutions or with random fluctuations in mutation frequencies. Interestingly, we identified mutants that acquired potential N-linked glycosylation sites in residues that represent novel locations for glycosylation in H1 viruses (Das et al., 2010). Two of the residues occupy surface locations that could accommodate an

oligosaccharide (93, 172), while the third residue (210) is located on the interior of the trimer where oligosaccharide addition would likely interfere with trimer formation. Given the fitness costs associated with adding novel oligosaccharides (Das et al., 2011), it will be interesting in future studies to characterize these variants biochemically and functionally.

The critical finding is that even among the more abundant mutants, there were large or even absolute differences in their presence in WT versus SEQ-7 escape populations. Differences at four residues reached high statistical significance (Fisher's two tailed t test with Bonferroni correction for the number of residues queried) (Table 3). Three examples are particularly striking. Substitutions at residue 169 were present in 12% of WT variants but only 0.5% of SEQ-7 variants. Sixteen percent of WT variants had alterations at residue 207, while the lone mutant detected among nearly 200 SEQ-7 variants analyzed had a compensatory D225Y substitution, a residue known to modulate HA receptor avidity/specificity (Stevens et al., 2006). Conversely, none of the 200 hundred-plus WT mutants had substitutions at residue 225, which was represented in 18% of SEQ-7 mutants.

We extended these findings by using H17-L10 to select a repertoire of SEQ-8 escape mutants. Of escape variants, 12.5% and 10% exhibited alterations in residues 210 and 222, while mutation in these residues comprises less than 1% of WT and SEQ-7 escape repertoires. Seven other unique variants are present at low frequency in the SEQ-8 escape repertoire.

Taken together, these findings indicate that the escape mutant repertoire is greatly affected by the exact HA sequence in the globular domain. Substitution of even a single residue (E119K, in the Cb epitope) between SEQ-7 and SEQ-8 has a major effect on the repertoire of mutants that escape a mAb specific for a different antigenic site (Ca).

Ab Escape by IAV HA Is Context Dependent

To better understand how HA sequence influences the escape repertoire, we introduced D225Y into WT HA and S207P into the SEQ-7 HA using the PR8 pDZ reverse-genetics plasmid system (Quinlivan et al., 2005). The four viruses achieved similar titers in MDCK cells (Figures 4A–4C). Each of the mutants demonstrated reduced titers in eggs, however, with SEQ-7-S207P demonstrating a 6-$\log_{10}$ reduction in titer that accounts for its absence from the H17-L2/H17-L10 escape repertoire in egg grown virus stocks. The difference in growth in egg versus MDCK cells is likely due to alterations in HA receptor specificity.

By contrast, the effect of D225Y on PR8 growth in eggs, though statistically significant, was relatively minor, and its subdetectable frequency in virus stocks is due to another factor. As seen in Figures 4D and 4E, this substitution decreases the Ab binding affinity of H17-L10 or H17-L2 for PR8 by only ~2-fold. Although these mAbs bind equally or even more avidly to SEQ-7, D225Y reduces mAb binding at least 1,000-fold, typical for escape mutants (Frankel and Gerhard, 1979).

Based on these findings, we conclude that two important factors sculpting HA mutation space, HA functionality and antigenicity, are exquisitely influenced by the existing sequence. S207P illustrates an example of where an amino substitution compromises the function of HA in the context of WT PR8 (but not SEQ-7) in a host cell-dependent manner (growth in eggs being severely compromised), while D225Y induces a major antigenic alteration in the Ca antigenic site in the context of SEQ-7, but not WT PR8.

DISCUSSION

One of the most puzzling features of HA antigenic drift is the “linear” nature of HA evolution (Ito et al., 2011; Pybus and Rambaut, 2009). At any one time, isolates populating numerous evolutionary branches cocirculate in humans. Over a relatively short interval, selected isolates predominate to form the major evolutionary tree. This is consistent with the idea that relatively subtle mutations in HA confer large selective advantages.

Mathematical analysis and modeling provides enormous insight into HA evolution, but relies on a limited appreciation of the selective forces for amino acid substitutions as it focuses on antigenicity and receptor binding based on the location of the residue in defined antigenic or receptor binding sites (Ferguson et al., 2003; Ito et al., 2011; Koelle et al., 2006; Rambaut et al., 2008). A more complete understanding of HA evolution will entail considering the influence of amino acid substitutions acting at a distance on HA antigenicity and receptor binding, as well as the effects of mutations on other aspects of HA function, including membrane fusion activity and interaction with NA (Hensley et al., 2011; Kryazhimskiy et al., 2011) and other viral and host gene products (Tate et al., 2011).

Here, to better understand HA evolution, we sequentially selected virus with a series of mAbs until HA demonstrated a physiologically significant decrease in binding affinities with members of a very large panel of mAbs that neutralize the parent virus. We find that 12 mutations are required to “completely” abrogate antigenicity by these criteria, though it is important to recognize the escape is a continuous and not quantal process; escape mutants will no longer escape given sufficiently high concentrations of neutralizing Abs. Definitive evidence that SEQ-12 effectively escapes immunity comes from in vivo competition experiments, where in a single passage in immune mice SEQ-12 outcompetes WT virus despite starting as a minor population.

Notably, we encountered no obvious bottlenecks during the sequential selection process, as mutants were obtained at each step at typical frequencies. It is clear from the rate of IAV evolution in nature and the very existence of 17 distinct subtypes that HA is capable of accommodating a large variety of amino acid substitutions and maintain not only function but also a remarkably similar structure. This in itself is not unusual; nearly all virus families demonstrate high sequence diversity yet maintain structure/function conservation in their attachment proteins, when considering all the serotypes that have evolved. The essential feature of antigenic plasticity is not the *degree* of diversity but how *rapidly* diversity can be achieved. As proteins mutate, they explore new fitness landscapes, and over an extended period, high diversity may be achieved as epistatic mutations restore function.

A critical question to be addressed in future studies is whether other viral glycoproteins exhibit similar plasticity to HA. It will be particularly interesting to compare HA to the functionally similar paramyxovirus HN which demonstrates a similar frequency of single escape variants (van Wyke Coelingh et al., 1987; Yewdell and Gerhard, 1982) yet evolves much more slowly than HA in nature.

Although variants were easily obtained at each selection step, sequencing revealed a remarkable epistatic change that occurred at the eighth selection step, where E119K was accompanied by an amino acid substitution in NA. The occurrence and fixation of the NA mutation correlated with increased avidity of HA for cellular receptors as measured by binding to progressively desialylated RBCs. In the simplest circumstances, NA activity would reverse mirror HA activity, as we have previously noted (Das et al., 2011; Hensley et al., 2011), but in this case the opposite occurred: the NA mutation reduced the amount of NA incorporated per virion, while HA demonstrated increased capacity to bind progressively desialylated RBCs. This emphasizes that the assays we use to measure HA

and NA function are imprecise proxies for their natural functions, and caution against oversimplifying our concepts of HA and NA cooperativity, which ultimately may include yet-undefined functions of each of these gene products.

Presumably, epistasis in NA occurs often during HA evolution, and accounts for a substantial fraction of NA variation. NA-HA epistasis suggests another possible reason for rapid antigenic drift in IAV compared to other RNA viruses: IAV has evolved to cushion alterations in HA function by compensatory changes in NA. This process might be further facilitated by the segmented nature of the IAV genome, which allows extremely rapid reassortment and rescue by gene segments under conditions of multiple infections (Nelson et al., 2008). Although the SEQ variants exhibited no coding changes in other genes, it is possible that HA also interacts with other viral gene products, e.g. M1 or M2, that exert epistatic effects.

We show that HA gradually changes its antigenicity with each selection step, indicating that the effects of amino acid substitutions on antigenicity are highly local. This is expected from the high structural conservation between WT and escape mutant HAs (Knossow et al., 1984), and particularly between widely divergent HA subtypes (Gamblin and Skehel, 2010). It is important to note that it is not possible to categorically determine the minimal alterations in HA required for escape from neutralizing Abs, since this is dependent on the exact composition and amounts of Abs present at the point of neutralization in vivo. This will vary enormously based on genetic differences between individuals, and particularly on their prior exposure to various HAs present in vaccines and natural infections. Thus, given an immunodominant response to a single antigenic site and a substitution that reduces the affinity of large majority of Abs specific for the site, even a single substitution can potentially provide some measure of escape (Jin et al., 2005; Natali et al., 1984; Smith et al., 2004), though the Ab response would likely have to be relatively weak (Cleveland et al., 1997; Cobey and Pascual, 2011). We also note that it is likely that with the proper mixture of mAbs specific for a single site, single amino acid substitutions could be identified that have maximal effects on site antigenicity, reducing the total number of mutations required to reach the antigenic distance from WT HA achieved by SEQ-12.

It is important to appreciate the highly conditional nature of antigenicity. We show that D225Y substitution in the context of WT HA has a 2-fold effect on the avidity of two mAbs, while diminishing avidity more than 1,000-fold in the context of SEQ-7. Extending these findings to epidemic viruses, E190D or Q197R substitutions selected for H17-L10 neutralization resistance in WT PR8 do not substantially reduce H17-L10 binding in the context of A/Bellamy/42 (which possesses E190D) or A/BH/1935 (which possesses A197R) (http://www.ncbi.nlm.nih.gov/genomes/FLU/flubiology.html) (Gerhard et al., 1981).

This means that great care must be taken in extrapolating the effects of amino acid substitutions on antigenicity; clearly context can dictate the outcome. Indeed, the importance of context is the critical finding of our study: the precise sequence of HA influences the effects of amino acid substitutions on HA antigenicity (a single amino acid change between SEQ-7 and SEQ-8 changes the repertoire of escape mutants) and also dictates the mutation space for further substitutions, as shown by the poor growth of the S207P in the context SEQ-7 replicating in MDCK cells.

Given the large number of highly variable residues in HA that can potentially influence the mutation fitness landscape, this casts doubts on the possibility of confidently predicting HA evolution in nature, a problem exacerbated by context-specific effects on antigenicity. All the more reason to focus efforts on developing vaccines targeted to conserved antigenic sites on HA (Han and Marasco, 2011; Kaur et al., 2011; Yewdell, 2011).

EXPERIMENTAL PROCEDURES

Virus

PR8 (originally obtained from Mount Sinai School of Medicine, New York, NY) and mutants were grown in allantoic cavities of embryonated hen eggs and were purified by differential centrifugation.

Hybridoma Abs

Hybridoma anti-HA Abs were produced and characterized as previously described (Caton et al., 1982; Gerhard et al., 1981; Staudt and Gerhard, 1983; Yewdell, 1981).

Variant Selection

Variants were selected by using the allantoison-shell (AOS) culture system or MDCK culture systems. Variant selection in AOS culture was done as described before (Gerhard et al., 1981). MDCK cells were seeded in 96-well plates (50,000 cells per well) and cultured for 16–24 hrs. Virus was serially diluted 10 fold (10^{-1} to 10^{-8}) at 50 μl/well in a parallel 96 plate. An equal volume of an overneutralizing concentration of mAb was added to each well, and the mixture was incubated at room temperature for 1 hr before adding to MDCK cells. After 2 hr at 37°C, cells were washed with PBS and replenished with 200 μl of media supplemented with 1 μg/ml TPCK trypsin and the selecting mAb. Cytopathic effect (CPE) was monitored 72–96 hr postinfection. Supernatants from CPE-positive wells (endpoint titer) were isolated for further amplification and characterization. Variants frequencies were determined as described elsewhere (Yewdell et al., 1986).

Radioimmunoassays

RIAs were performed as previously described (Gerhard et al., 1981) using detergent-disrupted virus adsorbed to 96-well polyvinyl microtiter plates and ^{125}I-labeled rabbit anti-mouse F(ab)′ 2 to detect bound Ab.

Virus ELISA

96-well plates (Immunlon 4HBX) were coated overnight at 4°C with saturating amounts of virus in allantoic fluid, then washed three times with PBS containing 0.05% v/v Tween-20, and blocked with PBS with 7.5% FBS for 1 hr. Abs present in culture fluid or ascites fluids over a complete range of dilutions from nondetectable to saturating binding were added for 2 hr at room temperature. After washing, 100 μl TMB substrate (KPL Biomedical) was added. The reaction was stopped by the addition of 50 μl of 0.1 N HCl, and the amount of product was determined by ELISA plate reader. Ab concentrations were determined by competition ELISA using purified mAbs as standards. Ab avidities were determined using Prism software, and all avidities reported demonstrated excellent fit for one site binding with Hill slope curve fitting (R^2 values > 0.98).

HI Assay, Virus Neutralization Assays

HI assays were performed in round-bottom 96-well polystyrene microtiter plates as previously described (Hensley et al., 2009). Virus neutralization assays were performed as described (Hensley et al., 2009). Each assay was repeated at least three times with three to five replicates per assay.

NA Assay

NA activity was determined as previously described (Hensley et al., 2011). Purified virus doses were adjusted for NA levels as determined by ELISA (for each virus, this

corresponded to ~50–100 HAUs of virus/sample). Viruses were diluted in assay dilution buffer (33 mM MES [pH 6.5], 4 mM CaCl2) with 200 uM of 29-4-methylumbelliferyl-alpha-D-N-acetyneuraminic acid. Samples were placed in black flat-bottom plates at 37°C, and OD (Ex = 365 nm; Em = 450 nm) readings were recorded every minute for 30 min. Data are expressed as the rate of enzymatic activity (relative Vmax). For some experiments, viruses were preincubated with 1% Triton-X to disrupt viral membranes. For some experiments, results were normalized based on relative NA protein concentration determined by quantitative western blot.

Virion Protein Content Analysis

Virus preps were boiled in the presence of DTT, resolved by polyacrylamide gel electrophoresis, and transferred to PVDF membranes. Blots were stained with mouse anti-HA2 mAb RA5-22 and rabbit anti-NA C terminus pAb, both of which target epitopes that are conserved between all sequential variants. Blots were then probed with IRDye 680 nm and 800 nm conjugated secondary Abs (Li-Cor) and simultaneously visualized and quantitated on an Odyssey infrared scanner using Image Studio v2.0 software (Li-Cor).

RNA Sequencing

Viral RNA was isolated from MDCK supernatant (endpoint titrated viruses and stocks) or allantoic fluid using QiAmp viral RNA mini kit (Qiagen) by using the manufacturer's protocol. cDNA was synthesized using a one-step reverse transcriptase kit (Origene Technologies). Gene-specific primers (PR8 HA-F, 5′-ATGAAGGCAAACCTACTGGTCCTG-3′; PR8 HA1-R, 5′-CTGCATAGCCT GATCCCTGTT-3′) amplified HA1, the PCR products were purified with a QIAQuick PCR purification kit (Qiagen), and sequencing was performed through a third-party sequencing service (MacrogenUSA) using dye-terminator cycle sequencing system with an ABI sequencer (Perkin-Elmer).

Generation of Recombinant Viruses

The recombinant WT and mutant viruses were generated by cotransfection of eight reverse-genetics plasmids containing the double-stranded DNA (dsDNA) representing each gene segment into 293T cells. Briefly, 2 μg of endotoxin-free ultrapure plasmid for each gene segment (total 16 μg) was mixed and transfected using calcium phosphate method to achieve ~90%–95% transfection efficiency. The supernatants were collected 48 hr posttransfection and treated with 10 μg/ml tosylsulfonyl phenylalanyl chloromethyl ketone (TPCK)-trypsin (Worthington, Lakewood, NJ) for 1 hr at 37°C. TPCK-trypsin-treated viruses were either infected to overnight grown MDCK cells (P_1-M passage) or 10-day-old embryonated eggs (P_1-E passage). Virus from 293T cells, MDCK cells, and eggs was titered by $TCID_{50}$ in MDCK cells.

In Vivo Challenge Experiment

For vaccine stocks, allantoic fluid was incubated with 0.05% paraformaldehyde for 2 days at 4°C. Mice were injected intraperitoneally with 2,000 HAU of inactivated influenza A viruses. Three weeks after vaccination, naive and immunized mice were tail vein bled, and sera was RDE treated overnight at 37°C, inactivated by incubating at 56°C for 30 min, and tested for anti-IAV Abs by HAI using turkey erythrocytes. Naive and vaccinated mice (five per group) were anesthetized with isoflurane and infected intranasally with $10^{4.8}$ $TCID_{50}$ units each of a mixture of PR8 and SEQ-12 viruses diluted in 50 ul BSS + 0.1% BSA. Lungs isolated 2 days after infection were homogenized and viral titers determined by endpoint dilution in MDCK cells. The relative abundance of PR8 and SEQ-12 variants was determined by sequencing a portion of the HA gene of plaque-cloned viruses from each

mouse lung. All mouse experiments were conducted in accordance with the guidelines of the NIAID Institutional Animal Care and Use Committee.

Supplementary Material

Refer to Web version on PubMed Central for supplementary material.

Acknowledgments

We thank Glennys Reynoso for providing outstanding technical assistance. We thank Dr. Walter Gerhard for his generous gift of the large panel of mAbs and viruses. We thank Dr. Adolfo Garcia-Sastre and Dr. David Wentworth for kindly providing eight-plasmid reverse-genetics plasmid to rescue WT and mutant viruses. We thank Dr. Zhiping Ye for providing ferret anti-sera to PR8 virus. The sequencing of the whole genome of the SEQ- variants was done at JCVI, which is one of the Genomic Sequencing Center of Infectious Diseases (GSCID) and has been funded with federal funds from the NIAID, NIH, and Department of Health and Human Services under contract number HHSN272200900007C. S.R.D. is supported by JCVI internal start-up fund. J.W.Y. and J.R.B. are generously supported by the Division of Intramural Research, NIAID. S.R.D., S.E.H., W.L.I., G.R., J.R.B., and J.W.Y. conceived of and designed experiments. S.R.D., S.E.H., W.L.I., C.B.B., A.S., M.G.D., G.R., and J.S.G. performed experiments. S.R.D., S.E.H., W.L.I., C.B.B., A.S., M.G.D., G.R., J.R.B., and J.W.Y. analyzed data. S.R.D. and J.W.Y. wrote the manuscript.

References

Caton AJ, Brownlee GG, Yewdell JW, Gerhard W. The antigenic structure of the influenza virus A/PR/8/34 hemagglutinin (H1 subtype). Cell. 1982; 31:417–427. [PubMed: 6186384]

Cleveland SM, Taylor HP, Dimmock NJ. Selection of neutralizing antibody escape mutants with type A influenza virus HA-specific polyclonal antisera: possible significance for antigenic drift. Epidemiol Infect. 1997; 118:149–154. [PubMed: 9129591]

Cobey S, Pascual M. Consequences of host heterogeneity, epitope immunodominance, and immune breadth for strain competition. J Theor Biol. 2011; 270:80–87. [PubMed: 21093455]

Das SR, Puigbò P, Hensley SE, Hurt DE, Bennink JR, Yewdell JW. Glycosylation focuses sequence variation in the influenza A virus H1 hemagglutinin globular domain. PLoS Pathog. 2010; 6:e1001211. http://dx.doi.org/10.1371/journal.ppat.1001211. [PubMed: 21124818]

Das SR, Hensley SE, David A, Schmidt L, Gibbs JS, Puigbò P, Ince WL, Bennink JR, Yewdell JW. Fitness costs limit influenza A virus hemagglutinin glycosylation as an immune evasion strategy. Proc Natl Acad Sci USA. 2011; 108:E1417–E1422. [PubMed: 22106257]

Ferguson NM, Galvani AP, Bush RM. Ecological and immunological determinants of influenza evolution. Nature. 2003; 422:428–433. [PubMed: 12660783]

Francis T Jr, Getting VA, et al. The present status of vaccination against influenza. Am J Public Health. 1947; 37:1109–1112.

Frankel ME, Gerhard W. The rapid determination of binding constants for antiviral antibodies by a radioimmunoassay. An analysis of the interaction between hybridoma proteins and influenza virus. Mol Immunol. 1979; 16:101–106. [PubMed: 447371]

Gamblin SJ, Skehel JJ. Influenza hemagglutinin and neuraminidase membrane glycoproteins. J Biol Chem. 2010; 285:28403–28409. [PubMed: 20538598]

Gerhard W, Yewdell J, Frankel ME, Webster R. Antigenic structure of influenza virus haemagglutinin defined by hybridoma antibodies. Nature. 1981; 290:713–717. [PubMed: 6163993]

Han T, Marasco WA. Structural basis of influenza virus neutralization. Ann N Y Acad Sci. 2011; 1217:178–190. [PubMed: 21251008]

Hensley SE, Das SR, Bailey AL, Schmidt LM, Hickman HD, Jayaraman A, Viswanathan K, Raman R, Sasisekharan R, Bennink JR, Yewdell JW. Hemagglutinin receptor binding avidity drives influenza A virus antigenic drift. Science. 2009; 326:734–736. [PubMed: 19900932]

Hensley SE, Das SR, Gibbs JS, Bailey AL, Schmidt LM, Bennink JR, Yewdell JW. Influenza A virus hemagglutinin antibody escape promotes neuraminidase antigenic variation and drug resistance. PLoS ONE. 2011; 6:e15190. http://dx.doi.org/10.1371/journal.pone.0015190. [PubMed: 21364978]

Ito K, Igarashi M, Miyazaki Y, Murakami T, Iida S, Kida H, Takada A. Gnarled-trunk evolutionary model of influenza A virus hemagglutinin. PLoS ONE. 2011; 6:e25953. http://dx.doi.org/10.1371/journal.pone.0025953. [PubMed: 22028800]

Jin H, Zhou H, Liu H, Chan W, Adhikary L, Mahmood K, Lee MS, Kemble G. Two residues in the hemagglutinin of A/Fujian/411/02-like influenza viruses are responsible for antigenic drift from A/Panama/2007/99. Virology. 2005; 336:113–119. [PubMed: 15866076]

Kaur K, Sullivan M, Wilson PC. Targeting B cell responses in universal influenza vaccine design. Trends Immunol. 2011; 32:524–531. [PubMed: 21940217]

Knossow M, Daniels RS, Douglas AR, Skehel JJ, Wiley DC. Three-dimensional structure of an antigenic mutant of the influenza virus haemagglutinin. Nature. 1984; 311:678–680. [PubMed: 6207440]

Koelle K, Cobey S, Grenfell B, Pascual M. Epochal evolution shapes the phylodynamics of interpandemic influenza A (H3N2) in humans. Science. 2006; 314:1898–1903. [PubMed: 17185596]

Kryazhimskiy S, Dushoff J, Bazykin GA, Plotkin JB. Prevalence of epistasis in the evolution of influenza A surface proteins. PLoS Genet. 2011; 7:e1001301. http://dx.doi.org/10.1371/journal.pgen.1001301. [PubMed: 21390205]

Molinari NAM, Ortega-Sanchez IR, Messonnier ML, Thompson WW, Wortley PM, Weintraub E, Bridges CB. The annual impact of seasonal influenza in the US: measuring disease burden and costs. Vaccine. 2007; 25:5086–5096. [PubMed: 17544181]

Natali A, Panizzi PF, Chezzi C, Oxford JS. Human sera possess a limited antibody repertoire to influenza neuraminidase antigenic variants selected in vitro. J Hyg (Lond). 1984; 92:243–250. [PubMed: 6707473]

Nelson MI, Viboud C, Simonsen L, Bennett RT, Griesemer SB, St George K, Taylor J, Spiro DJ, Sengamalay NA, Ghedin E, et al. Multiple reassortment events in the evolutionary history of H1N1 influenza A virus since 1918. PLoS Pathog. 2008; 4:e1000012. http://dx.doi.org/10.1371/journal.ppat.1000012. [PubMed: 18463694]

Pybus OG, Rambaut A. Evolutionary analysis of the dynamics of viral infectious disease. Nat Rev Genet. 2009; 10:540–550. [PubMed: 19564871]

Quinlivan M, Zamarin D, García-Sastre A, Cullinane A, Chambers T, Palese P. Attenuation of equine influenza viruses through truncations of the NS1 protein. J Virol. 2005; 79:8431–8439. [PubMed: 15956587]

Rambaut A, Pybus OG, Nelson MI, Viboud C, Taubenberger JK, Holmes EC. The genomic and epidemiological dynamics of human influenza A virus. Nature. 2008; 453:615–619. [PubMed: 18418375]

Smith DJ, Lapedes AS, de Jong JC, Bestebroer TM, Rimmelzwaan GF, Osterhaus AD, Fouchier RA. Mapping the antigenic and genetic evolution of influenza virus. Science. 2004; 305:371–376. [PubMed: 15218094]

Staudt LM, Gerhard W. Generation of antibody diversity in the immune response of BALB/c mice to influenza virus hemagglutinin. I. Significant variation in repertoire expression between individual mice. J Exp Med. 1983; 157:687–704. [PubMed: 6600489]

Stevens J, Blixt O, Tumpey TM, Taubenberger JK, Paulson JC, Wilson IA. Structure and receptor specificity of the hemagglutinin from an H5N1 influenza virus. Science. 2006; 312:404–410. [PubMed: 16543414]

Tate MD, Brooks AG, Reading PC. Receptor specificity of the influenza virus hemagglutinin modulates sensitivity to soluble collectins of the innate immune system and virulence in mice. Virology. 2011; 413:128–138. [PubMed: 21419468]

van Wyke Coelingh KL, Winter CC, Jorgensen ED, Murphy BR. Antigenic and structural properties of the hemagglutinin-neuraminidase glycoprotein of human parainfluenza virus type 3: sequence analysis of variants selected with monoclonal antibodies which inhibit infectivity, hemagglutination, and neuraminidase activities. J Virol. 1987; 61:1473–1477. [PubMed: 2437318]

Webster, RG.; Laver, WG.; Kilbourne, ED. The Influenza Viruses and Influenza. New York: Academic Press; 1975. Antigenic variation of influenza viruses; p. 269-314.

Yewdell, JW. Immunology. Philadelphia: University of Pennsylvania; 1981. The study of influenza virus antigens by means of monoclonal hybridoma antibodies; p. 213

Yewdell JW. Viva la revolucion: rethinking influenza A virus antigenic drift. Curr Opin Virol. 2011; 1:177–183. [PubMed: 22034587]

Yewdell J, Gerhard W. Delineation of four antigenic sites on a paramyxovirus glycoprotein via which monoclonal antibodies mediate distinct antiviral activities. J Immunol. 1982; 128:2670–2675. [PubMed: 6281335]

Yewdell JW, Caton AJ, Gerhard W. Selection of influenza A virus adsorptive mutants by growth in the presence of a mixture of monoclonal antihemagglutinin antibodies. J Virol. 1986; 57:623–628. [PubMed: 2418215]

Yewdell JW, Yellen A, Bächi T. Monoclonal antibodies localize events in the folding, assembly, and intracellular transport of the influenza virus hemagglutinin glycoprotein. Cell. 1988; 52:843–852. [PubMed: 2450677]

Yewdell JW, Taylor A, Yellen A, Caton A, Gerhard W, Bächi T. Mutations in or near the fusion peptide of the influenza virus hemagglutinin affect an antigenic site in the globular region. J Virol. 1993; 67:933–942. [PubMed: 7678310]

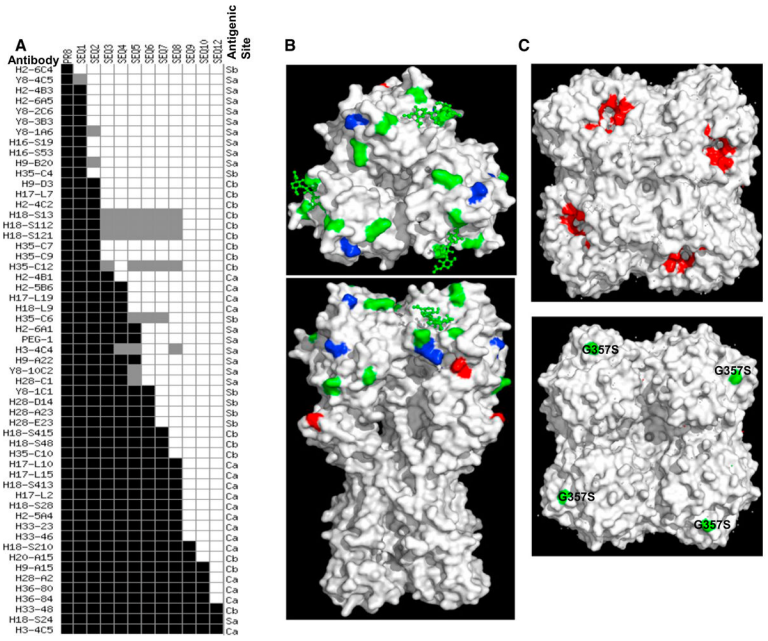

Figure 1. Antigenic Map of Sequential Variants

(A) The antigenicity of SEQ variants was determined by measuring the relative binding affinities of a panel of 60 mAbs via RIA. Black shows equivalent binding to mutant and WT viruses; gray shows reduced affinity (2- to 4-fold); white shows greatly reduced affinity.

(B) Three-dimensional model of HA rendered by PyMOL software as a solid surface looking at top and side of the trimeric molecule (using PR8 HA crystal structure 1RVX). Amino acid substitutions in escape mutants are indicated by color and label. Green shows same substitutions when selected with PR8, blue shows same amino acid position but a new substitution, and red shows new position.

(C) Three-dimensional model of NA rendered by PyMOL software as a solid surface looking at top (top panel) and membrane proximal (bottom panel) aspects of the tetramer molecule (using H5N1 NA crystal structure 2HTY). NA active sites (118, 151, 152, 224, 227, 276, 292, and 371) are labeled in red and substitution G357S (H5N1 NA crystal structure 2HTY numbering) that is present in SEQ-8, SEQ-9, and SEQ-10 and decreases NA activity in green.

Also see Figure S1.

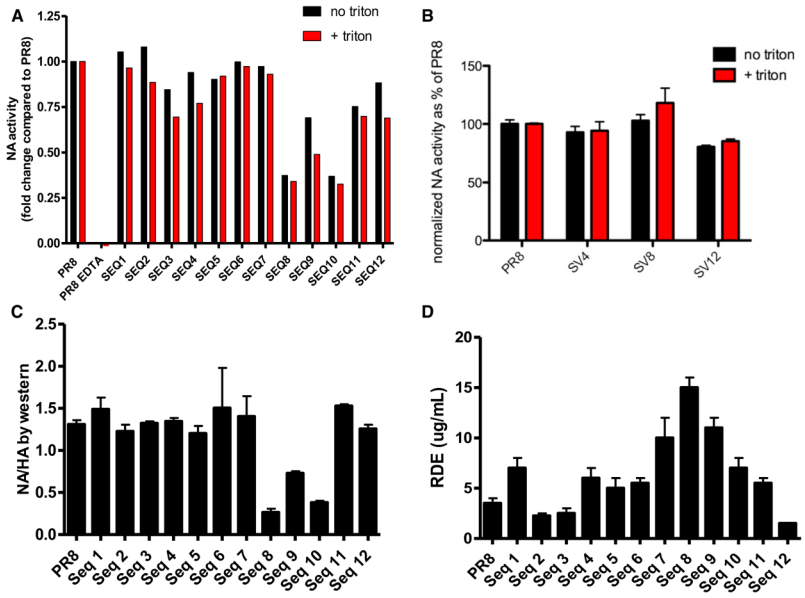

Figure 2. Sequential Variants Acquire Epistatic Changes in NA to Optimize Receptor Avidity

(A) NA activities of HAU-normalized viruses ± detergent to dissociate viral glycoproteins were determined using a small fluorogenic substrate.

(B) NA activities of PR8, SEQ-4, SEQ-8, and SEQ-12 normalized to the amount of NA protein in virions as determined by western blot.

(C) Ratios of NA/HA protein content in virions determined by immunoblotting.

(D) Receptor binding avidities of SEQ- variants were measured, determining the amount of RDE required to abrogate agglutination of turkey RBCs. Data are represented as mean ± SEM.

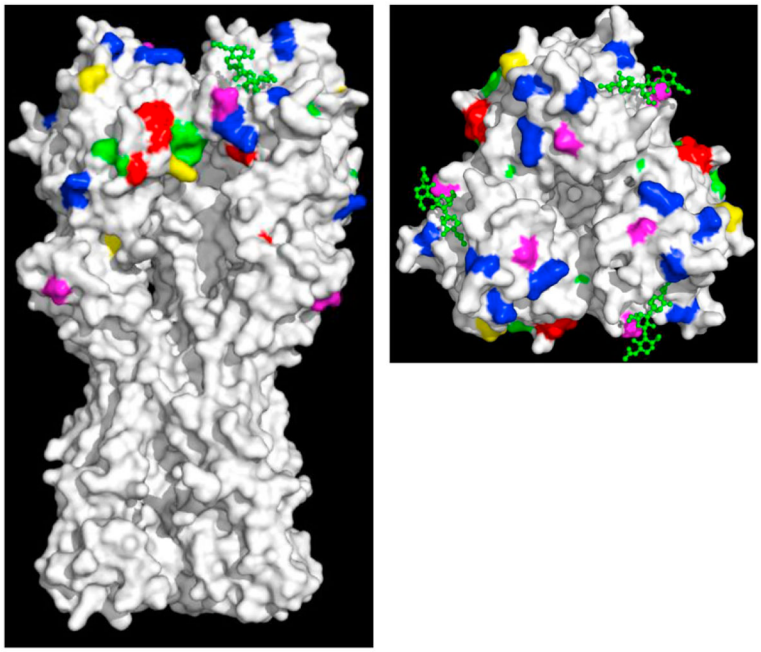

Figure 3. Locating H17-L2 and H17-L10 Escape Substitutions

Three-dimensional model of HA rendered by PyMOL software as a solid surface looking at top and side of the trimeric molecule (using PR8 HA crystal structure 1RVX). Amino acid substitutions in sequential variants are labeled in blue. Escape mutants of H17-L10 and H17-L2 that are present in both PR8 and SEQ-7 repertoire are labeled in red. Green shows substitutions exclusively in PR8 escape repertoire, magenta shows substitutions exclusively in SEQ-7 repertoire, and yellow shows substitutions exclusively in SEQ-8 repertoire. See also Table 3 and Table S3.

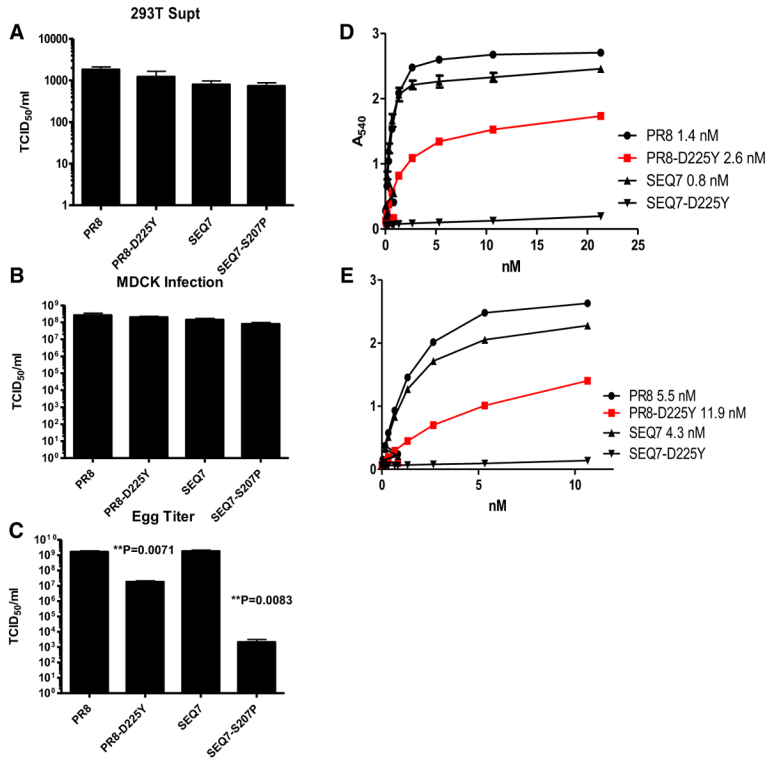

Figure 4. Antigenic Evolution Is Context Specific

(A) $TCID_{50}$ titers of WT and mutant viruses rescued (P_0 passage) after eight-plasmid transfection in 293T cells.

(B) $TCID_{50}$ titers of WT and mutant viruses rescued (P_1-M passage) after amplifying in MDCK cells.

(C) $TCID_{50}$ titers of WT and mutant viruses rescued (P_1-E passage) after amplifying in MDCK cells. All the experiments were performed in quadruplet, and the p values were calculated using Prism software (Student's t test).

(D and E) Binding affinities of H17-L10 and H17-L2 to PR8, PR8-D225Y, SEQ-7, and SEQ-7-D225Y were calculated by ELISA using detergent-disrupted viruses. All the experiments were done in quadruplicate, and dissociation constants were calculated using Prism software. All avidities reported demonstrated excellent fit for one site binding with Hill slope curve fitting (R^2 values > 0.98). Data are represented as mean ± SEM. See also Table S2.

Table 1

Selection of Sequential Variants

Sequential Variant	Antibody Used	Epitope	Antigenic Site	Substitution
SEQ-1	H2-6C4	B	Sb	**G159S**
SEQ-2	H2-4B3	C	Sa	**N129D**
SEQ-3	H9-D3	L	Cb	**R78G**
SEQ-4	H2-4B1	D	Ca1	**R224K**
SEQ-5	H2-5B6	N	Ca2	**S145N**
SEQ-6	H2-6A1	K	Sa	**K163E**
SEQ-7	Y8-1C1	E	Sb	**E156K**
SEQ-8	H18-S415	R	Cb	**E119K**
SEQ-9	H17-L10	S	Ca1	**G173R**
SEQ-10	H18-S210	T	Ca2	**E70G**
SEQ-11	H9-A15	M	Cb	**R48K**
SEQ-12	H36-80 & H36-84		Ca2	**D225G**

Table shows antibodies used to generate the sequential variants, their single-letter epitope designation, and location among the five antigenic sites in the globular domain. Substitutions in SEQ-1, SEQ-3, SEQ-5, SEQ-6, SEQ-7, SEQ-9, and SEQ-12 reiterate previously observed substitutions in PR8 mAb escape mutants, in SEQ-2, SEQ-4, and SEQ-8 novel amino acids in previously reported positions, and in SEQ-10 and SEQ-11 novel residues.

Table 2

mAbs Reactivity Parallels Functional pAb Recognition

		Mouse		Ferret Sera					
Virus	**Number mAb +**	**1°**	**2°**	**1**	**2**	**3**	**Guinea Pig**	**Rabbit**	**Chicken**
PR8	182 = 100%	1,750	1,750	2,560	1,280	320	320	160	1,280
SEQ-3	ND*	700	700	1280	ND	80	160	40	80
SEQ-6	ND*	200	200	320	ND	40	80	<10	40
SEQ-10	7%	110(6%)	110(6%)	ND	ND	40	20	<10	40
SEQ-12	2%	<30(<2%)	<30(<2%)	ND	40	40	10	<10	40

ND*, not done. WT or SEQ- mutants were tested for their binding to mAbs by indirect RIA and were scored for >10-fold decrease in affinity. By SEQ-12 all but four mAbs showed large affinity losses—the remaining four mAbs have low HI/VN activities. Viruses were also tested in standard HI assays against pooled Balb/c mouse primary or secondary sera (following i.p. PR8 infection), ferret sera from three animals (post-i.n. infection), pooled guinea pig sera (following i.n. infection), rabbit hyperimmune serum (following s.c. priming and boosting twice), and chicken serum. ND, not determined. Also see Table S1.

Table 3

Distinct WT versus SEQ-7 H17-L10 or H17-L2 Escape Repertoires

					T Test	
Sub	**WT**		**SEQ-7**		**WT SEQ-7**	**SEQ-8**
	H17-L10	**H17-L2**	**H17-10**	**H17-L2**		**H17-L10**
G50E[a]				1/89		
[gly]I93T	5/121	4/114		1/89		5/41
F99L[a]	1/121					
E124G[a]	1/121	3/114				
S125P						1/41
P127S[a]	1/114					
S140P[a]	1/121	1/114				
E142K[a]	4/121	2/114				
L152P	1/114					
V169A	4/121	9/114			<.0001	
E	1/121	2/114				
M	2/121	3/114		1/89		2/41
[gly]K172T	1/121[a]					2/41
G173R	20/121	19/114	5/103	5/89	<.0001	9/41
E	8/121	6/114	2/103	1/89		
W		2/114				
P186S[a]	7/121	5/114				
Q191T[a]						1/41
N197D				1/89		
T206I	1/121					
S207P	6/121	5/114		1/89[a]	<.0001	
L	11/121	17/114				
A						1/41

Sub	WT		SEQ-7		T Test WT SEQ-7	SEQ-8
	H17-L10	H17-L2	H17-10	H17-L2		H17-L10
N208S	1/121					
^{gly}N210S	1/121[a]					4/41
H						1/41
I217M[a]	1/121	1/114				
A218T	1/121					
E219K[a]				2/89		
K222Q[a]	1/121					3/41
V223R[a]	1/121					
R224K[a]	2/121					
D225Y			4/103	16/89	<.0001	
G			1/103	3/89		
T235N						1/41
K238T						1/41
G240R	36/121	34/114	84/103	50/89		2/41
E	16/121	1/114		3/89		5/41
N				1/103		
D241N	4/121	3/114				2/41
Y	2/121					
T242K	1/121	4/114	4/103	6/89		
I244M		1/114				
A247T[a]	1/121	1/114				
A253P				4/89		
T[a]				2/89		
Y256F[a]	1/114					
A257S[a]			1/103			

Sub	WT		SEQ-7		T Test WT SEQ-7	SEQ-8
	H17-L10	H17-L2	H17-10	H17-L2		H17-L10
A262K[a]	1/121	1/114	1/103	2/89		
S266N						1/41
G268R						1/41
S271L	1/121		1/103			
N279D			1/103			

Large panels of escape mutants were selected using PR8, SEQ-7, or SEQ-8 in presence of saturating amounts of H17-L10 or H17-L2 Abs. After sequencing, mutants were grouped based on the substitution in HA. **gly**Generates an additional glycosylation site (N-x-S/T, where x is any amino acid except P). P value from Fisher's two tailed t-test. With a Bonferroni correction of 23 residues at which substitutions occur, true significance at $p < 0.05$ must be corrected by dividing by 23, which = 0.002. For detail of the substitutions in each escape mutant, also see Figure 3 and Table S3.

[a]Only present as a double mutant, likely to represent an epistatic substitution to improve fitness of mAb escape.